Dendritic Aggregation of Oligothiophene during Desorption of 2,5-Diiodothiophene Multilayer and Topography-Induced Alignment of Oligothiophene Nanofibers

Guangming Liu,[†] Keith B. Rider,[‡] Wook-Jun Nam,[§] Stephen J. Fonash,[§] and Seong H. Kim*,[†]

Department of Chemical Engineering and Center for Nanotechnology Education and Utilization, The Pennsylvania State University, University Park, Pennsylvania 16802-4400, and Department of Natural Science, Longwood University, Farmville, Virginia 23909

Received: May 31, 2006; In Final Form: July 25, 2006

The multilayer desorption behavior of 2,5-diidothiophene and the dendritic aggregation of photochemical reaction products during the desorption of 2,5-diiodothiophene multilayers have been studied. Like many other aromatic compounds, 2,5-diiodothiophene shows a multilayer desorption behavior different from the typical zeroth-order kinetics, a metastable desorption peak growth at ∼220 K followed by a thick multilayer peak growth at ∼235 K. Traditionally, these desorption behaviors have been attributed to the formation of three-dimensional clusters. This paper provides the direct evidence of this clustering process by producing nondesorbing photoreaction products in the multilayer and by imaging their clusters after the multilayer desorption. Oligothiophene species are produced via photochemical reactions of 2,5-diiodothiophene during the multilayer deposition at ∼180 K in ultrahigh vacuum (UHV). Upon heating the multilayer to room temperature, the oligothiophene species forms into fibrous aggregates with a fractal dimension varying from 1.37 to 1.81 depending on their surface concentration. Using a topographical alteration of the substrate with a repeating pattern, these oligothiophene fibers can be aligned to a certain direction. This may allow in-situ fabrication of aligned conjugated polymer fibers directly on a target substrate.

I. Introduction

The study of reactions of organic molecules adsorbed on solid surfaces has traditionally focused on the first one or two monolayers on the surface.[1,2] Recently, reactions in thick multilayers are receiving considerable attention because of their potential applications to in-situ fabrication of functional organic structures on device surfaces. A specific interest is given to the possibility of producing conjugated polymer structures via photochemical reactions in multilayers of the monolayer species adsorbed or condensed on the substrate surface at a cryogenic temperature in ultrahigh vacuum (UHV) conditions.[3−5] This paper presents the effect of the multilayer desorption behavior of the unreacted monomer species on the aggregation and nanostructure formation of the photoreaction products.

Multilayers of aromatic and heteroaromatic compounds often exhibit complicated desorption behaviors deviating from simple zeroth-order desorption kinetics.[6−9] For these systems, one or several metastable desorption peaks are typically observed before one dominant multilayer desorption peak grows in temperature-programmed desorption (TPD). These behaviors have been attributed to a specific orientation of molecules in the second or third layers, transition from two-dimensional to three-dimensional clusters, metastable or semicrystalline phases, and so forth. Although there is much spectroscopic evidence of these changes, how these processes affect the morphology of reaction products when the samples are retrieved to the ambient condition has not been extensively studied. This is because the reaction products as well as the unreacted monomers are often desorbed in UHV before the substrate temperature reaches room temperature. The photopolymerization of adsorbed monomeric species provides a unique opportunity to study these effects since the polymerized reaction products do not desorb because of their high molecular weight. These products can be analyzed with nondestructive imaging techniques such as optical microscopy and scanning probe microscopy.

This paper presents the complicated desorption behavior of 2,5-diiodothiophene multilayers and dendritic aggregation of oligothiophene molecules photochemically produced inside the 2,5-diiodothiophene multilayer during the desorption of unreacted monomers. The multilayer desorption behavior was studied on a gold surface passivated with the reaction product of the 2,5-diiodothiophene and clean gold. As the multilayer thickness increases, a low-temperature peak grows first at ∼220 K and then a second peak grows at ∼235 K. On the basis of the peak shape, this change is due to a three-dimensional clustering of adsorbed molecules. This process was visualized by producing oligothiophene species during the multilayer desportion and by imaging their clusters with fluorescence microscopy after the multilayer desorption. The oligothiophene species were produced by UV irradiation during the multilayer deposition as well as desorption. UV irradiation of 2,5-diiodothiophene during the multilayer deposition can cause the photodissociation of C−I bonds in some molecules. The recombination of the produced thienyl radicals leads to formation of oligothiophene species.[5,10−13] On flat substrate surfaces, these oligothiophene species aggregate into randomly oriented dendritic structures with a fractal dimension varying from 1.37 to 1.81 depending on the surface concentration of oligothiophene species. These random dendritic

* Author to whom correspondence should be addressed. E-mail: shkim@engr.psu.edu.

[†] Department of Chemical Engineering, The Pennsylvania State University.

[‡] Longwood University.

[§] Center for Nanotechnology Education and Utilization, The Pennsylvania State University.

10.1021/jp063363f CCC: $33.50
Published on Web 09/09/2006

patterns can be aligned into a certain direction using topographical modification of the substrate surface.

II. Experimental Details

TPD of 2,5-diiodothiophene multilayer on gold was studied in a UHV chamber equipped with an Ar-ion sputter gun, a gas doser, a quadrupole mass spectrometer, an X-ray source, and a hemispherical energy analyzer. The base pressure of this UHV system was $\sim 1 \times 10^{-9}$ Torr and it further decreased to mid 10^{-10} Torr range with the sample manipulator cooled with liquid nitrogen. 2,5-Diiodothiophene was purchased from Aldrich (purity > 98%), purified by several freeze−pump−thaw cycles and was stored in a glass tube connected to the UHV chamber via a leak valve. A 0.25-in. stainless steel tube was attached to the leak valve exit for direct dose of 2,5-diiodothiophene to the substrate surface. The nominal exposure was calculated without considering the flux enhancement from the direct dose geometry. A gold foil was cleaned by Ar^+ ion sputtering and then was passivated by exposure to 2,5-diiodothiophene and was heated to 450 K. The passivation of the gold surface was monitored with X-ray photoelectron spectroscopy (XPS). The first monolayer of 2,5-diiodothiophene undergoes the C−I bond dissociation at 220∼300 K on a clean Au surface. Details of the first monolayer reaction will be published separately elsewhere.

The photochemical synthesis of oligothiophene was carried out in a separate UHV chamber equipped with a load-lock system for easy introduction and retrieval of samples. The base pressure of this system was $\sim 2 \times 10^{-9}$ Torr. A typical experimental procedure was as follows. A Au (70 nm) coated Si substrate was transferred to a sample holder in the UHV chamber. It was first sputter-cleaned with 2 keV Ar^+ ions for 30 min and then was cooled to ∼180 K by filling a coolant reservoir in contact with the sample holder with liquid nitrogen. The adsorption of residual background gases onto the cleaned surface at the dose temperature was not detectable with TPD and XPS. TPD results were obtained at a heating rate of 2 K/s.

For synthesis of oligothiophene, the clean Au substrate was exposed to 2×10^{-7} Torr 2,5-diiodothiophene and was simultaneously irradiated with a collimated UV light from a high-pressure mercury lamp. The UV lamp power was controlled between 40 and 200 W. The monomer dose time was varied from 20 to 60 min. After the simultaneous monomer dose and UV irradiation at 180 K, the leak valve was closed and the substrate was slowly warmed to room temperature (heating rate ∼ 4 K/min) while continuously irradiating with UV light. The substrate heating and postdose UV irradiation time was typically 30 min.

To study the topographic orientation effect on the aggregated oligothiophene species, a 20 μm × 30 μm area of parallel trench lines was made via a nanoimprint process. In this process, a mold structure was first fabricated into a 1-μm-thick thermal silicon oxide grown on a silicon substrate using electron beam lithography, lift-off, and dry-etching processes. After the mold fabrication, the pattern on the mold was printed into a 200-nm-thick poly(methyl methacrylate) (PMMA) film spin-coated on a silicon wafer. The PMMA film was baked at 140 °C for 3 min on a hot plate before imprinting. The mold and substrate were stacked together and loaded on an imprinting tool. The stack was pressed together at a temperature of 225 °C. After cooling to room temperature, the nanoimprinted substrate was separated from the mold and was coated with a 15-nm-thick gold film by thermal evaporation.

The produced oligothiophene samples were analyzed with reflection photoluminescence spectroscopy, near-edge X-ray absorption fine structure (NEXAFS), and X-ray diffraction (XRD). A single-monochromator spectrofluorometer was used with additional optical filters placed on both the excitation and emission side (excitation wavelength = 435 nm, emission wavelength = 450−800 nm) to remove the scattered light from the excitation monochromator source. An incidence angle of 80° with respect to surface normal was employed to characterize the oligothiophene species produced on the Au-coated Si surface. NEXAFS and XRD measurements were performed at the U1A and X18A beamline, respectively, of the National Synchrotron Radiation Source at the Brookhaven National Laboratory. The NEXAFS analysis was carried out for the C−K edge region to check if the produced oligothiophene contained any structural defects such as alkyl groups. The XRD measurements were made for the 2θ scan range from 3° to 23° under Ar purging conditions to prevent beam-induced damage to the polymer.

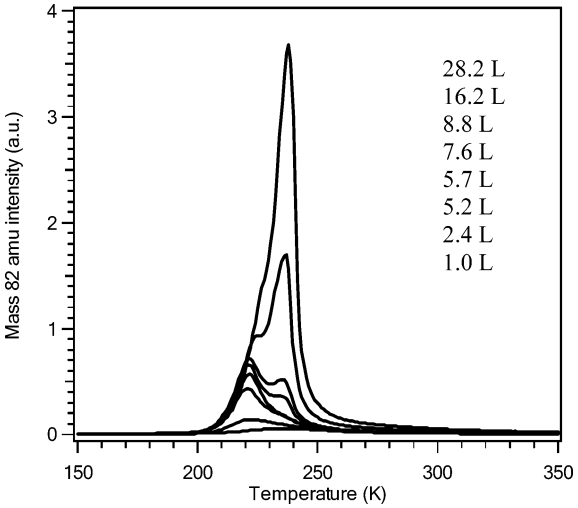

Figure 1. TPD results of 2,5-diiodothiophene multilayers on a passivated gold surface. The passivation was done by reacting the clean gold surface with 2,5-diiodothiophene. The exposure of 2,5-diiodothiophene was from 1 L (bottom) to 28 L (top).

The morphology of the produced oligothiophene was investigated with fluorescence microscopy and scanning electron microscopy (SEM). A fluorescence microscope (excitation source = 415−475 nm, emission filter = 525−700 nm) was used to image the photoluminescent polymer patterns on the substrate. SEM images were taken after depositing a ∼10-nm-thick gold film on the sample surface to prevent surface charging. The fractal dimension, f_D, of the produced oligothiophene aggregate species was determined by the box-counting analysis of the digitalized fluorescence microscopic images.[14] This method works by first covering the object with a grid of square boxes of size d and then counting the number of boxes, N_d, needed for complete coverage. The fractal dimension is calculated from the slope of a linear fit line in the ln N_d versus ln d^{-1} plot.

III. Results and Discussion

1. TPD of 2,5-Diiodothiophene Multilayer. The TPD data of 2,5-diiodothiophene multilayers on the passivated gold surface are shown in Figure 1. The reaction between the first monolayer and the clean gold surface leads to almost complete dissociation of the 2,5-diiodothiophene molecule. There was no detectable desorption species from the first monolayer until the substrate was heated to higher than 500 K. After complete passivation of the gold surface, the first multilayer desorption peak grows at ∼220 K. As the thickness of the multilayer increases, this

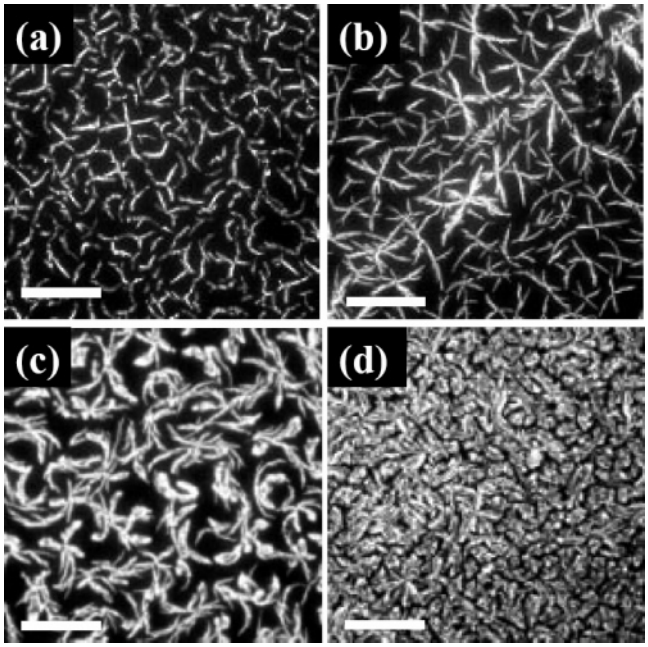

Figure 2. Fluorescence microscope images of oligothiophene films formed by photopolymerization of 2,5-diiodothiophene condensed at ~180 K on Au coated silicon wafer at different dosing times (dosing pressure = 2×10^{-7} Torr): (a) 20 min, (b) 35 min, (c) 48 min, (d) 60 min. The excitation and emission wavelengths of the filters used in fluorescence microscopy were 450 nm and 510−700 nm, respectively. The scale bar is 2 μm.

peak grows larger with a slight shift of its peak desorption to a higher temperature. However, the desorption peak profile of this peak does not follow the typical zeroth-order kinetics which shows the desorption rate being increased exponentially with the surface temperature and a sharp decrease to zero upon complete desorption of the multilayer. Instead, its desorption profile is more symmetric around the peak temperature. As the multilayer thickness is further increased, a second peak grows at ~235 K. The second peak grows faster than the first peak and eventually becomes dominant at high doses. The desorption profile of the second peak is slightly asymmetric at the peak position. This is much closer to the zeroth-order kinetics, although the exact profile still deviates from it.

This deviation behavior from the zeroth-order desorption kinetics can be explained with formation of three-dimensional clusters during desorption.[15] When the clusters are formed, the effective surface area of the adsorbate−vacuum interface changes as the monomer desorption occurs. The interface area decreases with two-thirds power of the remaining volume of the adsorbate, and the measured signal TPD intensity is the desorption rate at a given temperature times the total surface area of the clusters on the substrate. The former increases exponentially with the substrate temperature, but the latter decreases as the molecules desorb with the temperature rise. The product of these two terms produces a peak shape more symmetric than the typical zeroth-order multilayer desorption kinetics.

2. Dendritic Aggregation during the 2,5-Diiodothiophene Multilayer Desorption. When a fraction of adsorbate molecules in the multilayer are converted to polymeric nondesorbing species, the clustering process can be visualized by imaging the polymeric species after the complete desorption of the unreacted molecules. The degree of photoinduced reaction was kept low so that the 2,5-diiodothiophene multilayer was formed and dominated the desorption behavior of the condensed film. Figure 2 displays fluorescence microscopic images of oligothiophene species produced during the multilayer deposition and aggregated during the multilayer desorption. At a low concentration of the oligothiophene species (Figure 2a), plus-shaped dendritic fibers are exclusively formed. The thinnest fibers observed at the lowest oligothiophene coverage were about 80 nm in width and about 2 μm in length. The individual fiber width and length can increase to ~500 nm and ~10 μm, respectively, depending on the growth condition (SEM images shown in the Supporting Information). When the surface coverage of oligothiophene species is slightly increased, short branches are formed on the side of long fibers, producing a featherlike shape (Figure 2b). As the oligothiophene concentration is further increased, the produced patterns progress to highly curved multifiber aggregates with dendritic open structures (Figure 2c) and eventually to almost completely covered patches (Figure 2d). Upon close examinations, these patches are found to be composed of thin and curved fibrils.

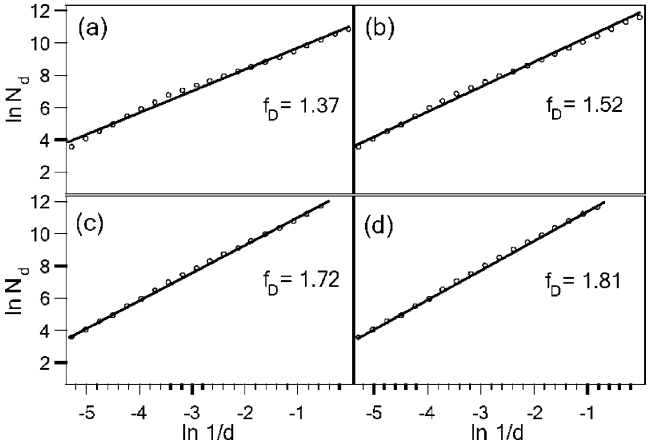

Figure 3. Box-counting analysis of the fractal dimensions of the patterns shown in Figure 2. The slope of a linear correlation fit line is the fractal dimension.

Although there are no distinct recurring patterns, there are significant similarities in each aggregate image shown in Figure 2. To distinguish the self-similarity between different oligothiophene concentration images,[16−18] the fractal dimension f_D of each image was analyzed with the box-counting method (Figure 3). The plus-shape fibrils observed at the lowest coverage (Figure 2a) show a fractal dimension of 1.37. The f_D value of 1.37 is within the typical fractal dimension range observed for diffusion-limited aggregation (DLA) processes.[16,19] In the DLA model, the unit species randomly diffuses until it comes into contact with a growing aggregate and sticks right at the initial contact position. The aggregates generated by this process are highly ramified because the fast-growing outer parts make the inner parts inaccessible for incoming particles.[20] In the unreacted 2,5-diiodothiophene multilayer, the oligothiophene species can diffuse in the multilayer film during the clustering process which takes place just below the desorption temperature. However, it is not clear if the dendritic fibers are grown by the DLA mechanism or not. The fact that most of the aggregate features have the plus-shape dendritic feature may indicate that these features are grown outward from the nuclei with some geometric constraints.

As the concentration of the oligothiophene species on the surface increases, the fractal dimension f_D increases to 1.52 (Figure 2b), 1.72 (Figure 2c), and 1.81 (Figure 2d). The increase of the fractal dimension at a higher coverage appears to be due to aggregation of individual fibers.[21] There are still thin fibrillar features inside the large aggregate domains.

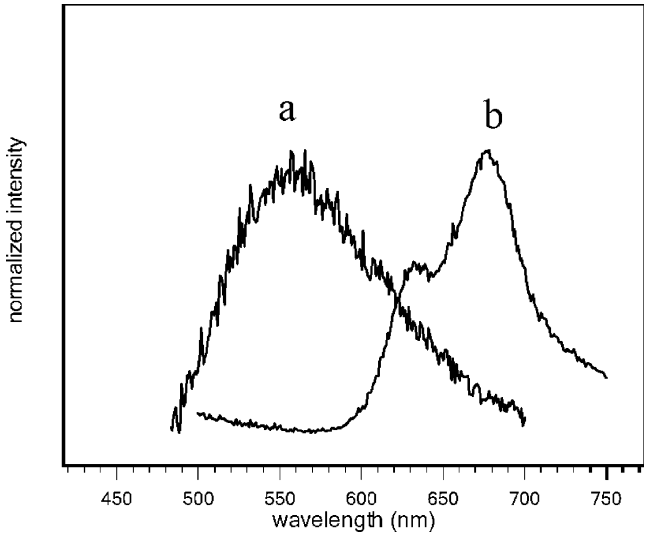

Figure 4. Reflection photoluminescence emission spectra of oligothiophene thin films. (a) Photopolymerized films composed of dendritic fibers and (b) chemically synthesized polythiophene reference film. The excitation wavelength was 435 nm in both cases.

3. Chemical Analysis of Oligothiophene Dendritic Aggregates. The conjugation length of the photochemically synthesized oligothiophene fibers is estimated with photoluminescence spectroscopy. Figure 4 compares the photoluminescence spectra for the photochemically synthesized sample in UHV and the chemically synthesized polythiophene (purchased from Aldrich). The emission maximum is 557 nm (green) for the UHV-produced sample and 677 nm (red) for the chemically synthesized polythiophene. The lower photoluminescence emission wavelength implies a shorter conjugation length. When compared to the literature, the average conjugation length is estimated to be 3−5 thiophene monomer units.[22] This result is in good agreement with our previous reflection absorption IR spectroscopy analysis for the oligothiophene thin films produced in a similar way in UHV.[5]

The NEXAFS spectra of the oligothiophene fibril samples are essentially the same as those for the UHV-synthesized oligothiophene thin films reported earlier.[5] There are two sharp transition peaks at 286.0 eV (C1s $\rightarrow \pi_1^*$) and at 287.7 eV (C1s $\rightarrow \sigma^*_{C-S}$), one shoulder peak at 289.0 eV (C1s $\rightarrow \pi_2^*$), and one broad transition at 295.0 eV (C1s $\rightarrow \sigma^*_{C-C}$). These are characteristic resonances of oligothiophene and polythiophene. There is no discernible peak around 292.5 eV associated with the σ^* (C−C) resonance of alkyl groups.

Synchrotron grazing-incidence XRD analysis was carried out to check if the oligothiophene molecules in the fibers are packed in an ordered structure. The XRD patterns of the oligothiophene film composed of fibers (Figure 5) exhibit two broad peaks at $2\theta = 4.3°$ (16.5 Å) and 4.7° (15.1 Å) and a very weak and broad shoulder at $2\theta = \sim 6.5°$. No other XRD patterns can be observed at $2\theta > 10°$. This XRD spectrum is very similar to those reported for chemically synthesized polythiophene powders.[23] These data imply that, although they are not crystalline, the samples have some degree of long-range order because of interchain interactions. Considering an elongated shape of oligothiophene molecules, a low degree of molecular packing order in the fibers seems reasonable.

4. Substrate Topography Induced Alignment of Oligothiophene Fibers. If fibrillar oligothiophene structures are produced via clustering during the desorption process of the unreacted monomer multilayer, one should be able to control the direction of the oligothiophene fibrils by growing those

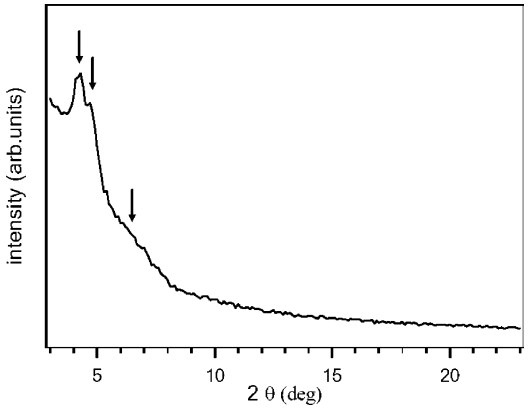

Figure 5. XRD spectra of ∼200-nm-thick oligothiophene thin film composed of dendritic fibers. The X-ray wavelength was 1.2399 Å. The arrows indicate XRD peaks showing at $2\theta = 4.3°$ (16.5 Å) and 4.7° (15.1 Å) and a broad shoulder at $2\theta = \sim 6.5°$.

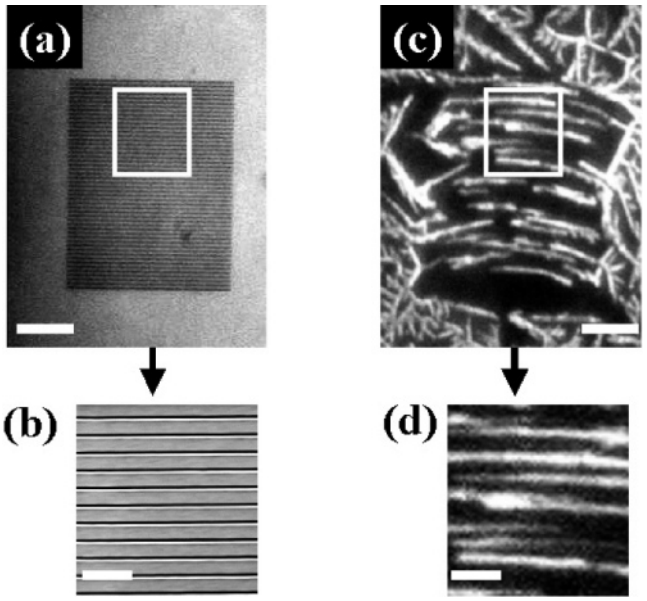

Figure 6. (a) Optical microscope image of a nanopatterned substrate of Au/PMMA/Si, nanoscale trench dimensions: width = 70 nm, depth = 200 nm, length = 30 μm; (b) FE-SEM image of the enlarged nanopattern region marked with a square in a; (c) fluorescence microscope image of the nanopatterned substrate region after dendritic growth of oligothiophene by photopolymerization in UHV; (d) enlarged fluorescence microscope image of the parallel oligothiophene fibers in the marked region in c. The scale bar in a and c is 10 μm. The scale bar in b and d is 2 μm.

structures on topographically modified or chemically heterogenized substrates. The chemically heterogenized surface is suitable for in-situ production of oligothiophene micropatterns.[13] In this paper, we describe the topographic modification approach to align oligothiophene submicrometer fibrils.

Using a nanoimprinting method, an array of parallel trench lines (∼70 nm wide, ∼200 nm deep, ∼30 μm long) is produced in a PMMA photoresist film and is coated with a 10-nm-thick gold film. Figure 6a and 6b displays the optical microscope and SEM images of the Au/PMMA/Si substrate with parallel lines of trenches, respectively. On this substrate, oligothiophene is produced photochemically during the deposition of 2,5-diiodothiophene multilayer and is allowed to aggregate during the desorption of the unreacted 2,5-diiodothiophene. Figure 6c exhibits the fluorescence micrograph of the produced oligothiophene fibers on and around the nanotrench array. In the growth condition used in this experiment (200 W UV irradiation

at a 2,5-diiodothiophene dosing pressure of 2×10^{-7} Torr for 30 min, followed by postdose UV irradiation during the sample heating), the width of the fibers is ~500 nm. As expected, the polymer fibers grown on the flat region (outside the nanotrench array) are highly branched and randomly oriented with a fractal dimension f_D of 1.67, similar to Figure 2b and 2c on the flat region. In contrast, a high degree of alignment can be seen for oligothiophene fibers grown on the nanotrench array region (Figure 6d). The aligned fibers appear to be bent slightly in the fluorescence microscope image, but this is due to the distortion of the underlying photoresist layer during the cooling and heating process (see optical microscope images in Supporting Information). This result indicates the aligning effect of the surface topography on the orientation of oligothiophene fibers produced in this process. Although the alignment mechanism is not fully understood yet, it is speculated that the alignment is either due to the confined diffusion of oligothiophene species in the nanotrench or is due to the dewetting of the multilayer film along the nanotrench direction during the clustering process. If a liquid phase of 2,5-diiodothiophene is formed before or during the thermal desorption, the surface tension of the liquid can cause the liquid to fill the trenches as the liquid volume decreases. This could alter diffusion of the radical or oligothiophene species. Another possible process during the multilayer dewetting is to align short oligothiophene fibers along the trench, making long fibers. More studies on the topography-induced nanofiber growth and alignment mechanisms are needed to get further insights.

To the best of our knowledge, there is no report of the in-situ directed growth of straight oligothiophene fibers using the technique of photopolymerization on a patterned substrate surface. This could be a new way of growing conjugated polymer fibers with controlled alignments. By combining the surface morphology and chemistry control methods with the photolithography technique, one could accomplish a higher level of spatial control.

IV. Conclusion

The clustering behavior during the multilayer desorption of 2,5-diiodothiophene is studied with TPD, and the dendritic aggregation of oligothiophene species photochemically produced from 2,5-diiodothiophene during the multilayer desorption is visualized using fluorescence microscopy. The morphology and fractal dimension of the dendritic aggregates imply that the oligothiophene fibrils are formed by the diffusion-limited aggregation process during the multilayer desorption of the unreacted molecules. These fibers aggregate as the oligothiophene species concentration increases on the substrate. The width of the fibers can vary in the range of 80~500 nm, depending on the growth conditions. By utilizing prefabricated nanopatterns on the substrate, these oligothiophene fibers can be aligned to a specific direction during the photochemical synthesis.

Acknowledgment. This work is supported by the American Chemical Society Petroleum Research Funds (PRF# 40605-G5) and the National Science Foundation (DMI-0210229). The authors appreciate Dr. Sergey Rykov at University of Delaware and Dr. Steven Ehrlich for their kind help with the use of U1a and X18a beamlines, respectively, at the National Synchrotron Radiation Source of the Brookhaven National Laboratory.

Supporting Information Available: SEM and bright-field images. This material is available free of charge via the Internet at http://pubs.acs.org.

References and Notes

(1) Street, S. C.; Xu, C.; Goodman, D. W. *Annu. Rev. Phys. Chem.* **1997**, *48*, 43−68.
(2) White, J. M. *Appl. Surf. Sci.* **1986**, *26* (4), 392−407.
(3) Hernandez, J. E.; Ahn, H.; Whitten, J. E. *J. Phys. Chem. B* **2001**, *105*, 8339−8344.
(4) Bai, J.; Snively, C.; Delgass, W. N.; Lauterbach, J. *Adv. Mater.* **2002**, *14* (21), 1546−1549.
(5) Liu, G.; Natarajan, S.; Kim, S. H. *Surf. Sci.* **2005**, *592*, L305.
(6) Eng, J., Jr.; Bent, B. E.; Fruhberger, B.; Chen, J. G. *J. Phys. Chem. B* **1997**, *101* (20), 4044−4054.
(7) Huang, W. X.; White, J. M. *J. Phys. Chem. B* **2004**, *108* (16), 5060−5065.
(8) Abdallah, W. A.; Nelson, A. E. *Surf. Sci.* **2005**, *585* (1−2), 113−122.
(9) Rockey, T. J.; Yang, M.; Dai, H. L. *Surf. Sci.* **2005**, *589* (1−3), 42−51.
(10) Natarajan, S.; Kim, S. H. *Thin Solid Films* **2006**, *496* (2), 606−611.
(11) Natarajan, S.; Kim, S. H. *Chem. Commun.* **2006**, *7*, 729−731.
(12) Natarajan, S.; Liu, G.; Kim, S. H. *J. Phys. Chem. B* **2006**, *110* (15), 8047−8051.
(13) Natarajan, S.; Kim, S. H. *Langmuir* **2005**, *21* (15), 7052−7056.
(14) Barabasi, A. L.; Stanley, H. E. *Fractal Concepts in Surface Growth*; University Press: Cambridge, U.K., 1995.
(15) Kim, S. H.; Stair, P. C.; Weitz, E. *Surf. Sci.* **2000**, *445*, 177.
(16) Witten, T. A.; Sander, L. M. *Phys. Rev. Lett.* **1981**, *47*, 1400.
(17) Witten, T. A.; Sander, L. M. *Phys. Rev. B* **1983**, *27*, 5686.
(18) Jelinek, H. F.; Fernandez, E. *J. Neurosci. Methods* **1998**, *81*, 9.
(19) Von Schulthess, G. K.; Benedek, G. B.; De Blois, R. W. *Macromolecules* **1980**, *13*, 939.
(20) Matsushita, M. In *The Fractal Approach to Heterogeneous Chemistry*; Avnir, D., Ed.; John Wiley and Sons Ltd.: New York, 1989.
(21) Radnoczi, G.; Vicsek, T.; Sander, L. M.; Grier, D. *Phys. Rev. A* **1987**, *35*, 4012.
(22) Fichou, D.; Ziegler, C. In *Handbook of Oligo- and Polythiophenes*; Fichou, D., Ed.; Wiley-VCH: Weinheim, Germany, 1999; p 183.
(23) Kanemitsu, Y.; Suzuki, K.; Shimizu, N.; Shiraishi, Y.; Kuroda, M. *Jpn. J. Appl. Phys.* **1996**, *35*, L1097.